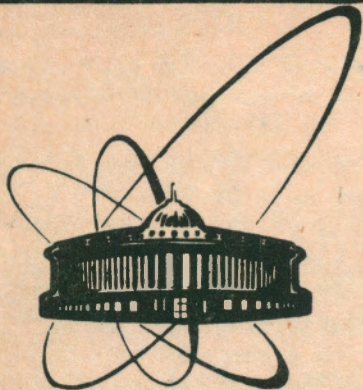


92-133



сообщения  
объединенного  
института  
ядерных  
исследований  
дубна

E1-92-133 *e*

Z.Strugalski, R.Bekmirzaev, N.Hassan<sup>1</sup>,  
E.Mulas<sup>2</sup>, T.Pawlak<sup>1</sup>, M.Sultanov<sup>3</sup>

THE MEAN CHARACTERISTICS OF THE PION  
PRODUCTION AND NUCLEON EMISSION PROCESSES  
IN PION-CARBON NUCLEAR COLLISIONS  
AT 40 GeV/c MOMENTUM

<sup>1</sup>Warsaw University of Technology, Institute of Physics,  
Warsaw, Poland

<sup>2</sup>Warsaw University of Technology, Plock, Poland

<sup>3</sup>Samarkand State University, Samarkand, Uzbekistan

1992

## 1. INTRODUCTION

This publication is the third one in the series of our works/<sup>1,2</sup> in which experimental data on hadron-<sup>12</sup>C<sub>6</sub> nuclear collisions are presented. The aim of these works has been to gain insight in the physics of the nucleon emission and pion production processes in hadron-nucleus collision reactions; the mean characteristics of the processes are here analysed predominantly.

The characteristics of the proton emission process are prepared in dependence on the multiplicity n<sub>pi</sub> of the produced pions in the collision reactions; the characteristics of the pion production process are prepared in dependence on the multiplicity n<sub>p</sub> of the emitted protons, the protons are emitted from the target nucleus in the collision reactions. The physical motivation for such a presentation is given in our former works/<sup>3,4</sup>.

## 2. EXPERIMENTAL PROCEDURE

The problems concerning the exposition of the 2 m propane bubble chamber to the beams of hadrons from the accelerators in Dubna, JINR and in Serpukhov, IHEP, as well as the chamber photographs analysis were discussed in the former works/<sup>1,2</sup> and in the works cited in them.

## 3. EXPERIMENTAL DATA

The experimental material was obtained in scanning the photographs of the JINR 2 m long propane bubble chamber exposed to pion beam at 40 GeV/c momentum from the Serpukhov, IHEP accelerator. Any of the pion-carbon nuclear collisions were looked for within the fiducial region inside the chamber, according to definite scanning criteria/<sup>5,6</sup>.

All the secondary particles in the pion-carbon collision reactions have been accepted to be pions, if not protons with

the momenta P<sub>lab</sub> 0.15 GeV/c  $\leq$  P<sub>lab</sub>  $\leq$  0.7 GeV/c. The admixture of the protons in the sample of the secondary positively charged particles is about 15%, in this case, the admixture of the K<sup>+</sup> mesons and  $\Sigma^{+}$  hyperons is no larger than/<sup>6</sup> 4-5%.

In this work 7577 Pi<sup>-</sup> + <sup>12</sup>C<sub>6</sub> collision events were selected. Mean characteristics of the pion production process were prepared in dependence on the multiplicity n<sub>pi</sub> of the emitted protons; the multiplicity n<sub>p</sub> indicates/<sup>1,2</sup> how thick layer of the intranuclear matter was involved in the collision reaction. Similarly, mean characteristics of the proton emission process were prepared in dependence on the pion production intensity in the collision events; the produced pion multiplicity n<sub>pi</sub> serves here as the measure of the pion production intensity.

Experimental data are presented on figs. 1, 2 and in the tables I-XII.

## 4. DISCUSSION AND RESULTS

A short conclusion review may be useful and give a summary of this work.

I. As it concerns the nucleon emission process:

1. The mean number  $\langle n_p \rangle$  of the protons in Pi<sup>-</sup> + <sup>12</sup>C<sub>6</sub> nuclear collisions in dependence on the intensity n<sub>pi</sub> of the produced pions changes from about 1.6 up to about 2; in average, the  $\langle n_p \rangle$  may be accepted as independent of the n<sub>pi</sub>, within the  $\langle n_p \rangle$  value change.

2. The mean number of the emitted protons,  $\langle n_p \rangle \approx 1.8$  protons, is near to the mean thickness  $\langle \lambda \rangle$  in protons/S of the carbon target nucleus  $\langle \lambda \rangle \cdot S \approx 1.5$  protons, where  $S = \pi D_0^2 \approx 10 \text{ fm}^2$  and D<sub>0</sub> is the diameter of the nucleon or the nuclear interaction range.

3. Mean momentum  $\langle P_{tot} \rangle$  and energy values  $\langle E_k \rangle$  of the emitted protons do not depend on the intensity n<sub>pi</sub> of the pion production in the collision reactions;  $\langle E_k \rangle = 60 \text{ MeV} \approx (m_{pi})/2$  and m<sub>pi</sub> is the pion rest mass.

4. In general, the mean values of the proton emission angles  $\langle \theta \rangle$  do not depend on the multiplicity n<sub>pi</sub> of the pion production in the hadron-nucleus collision reactions; the evidently different values of the  $\langle \cos \theta \rangle$  observed at n<sub>pi</sub> = 1 may correspond to the quasi-free collisions of the incident pion with a peripheral protons in the target nucleus.

II. As it concerns the pion production process:

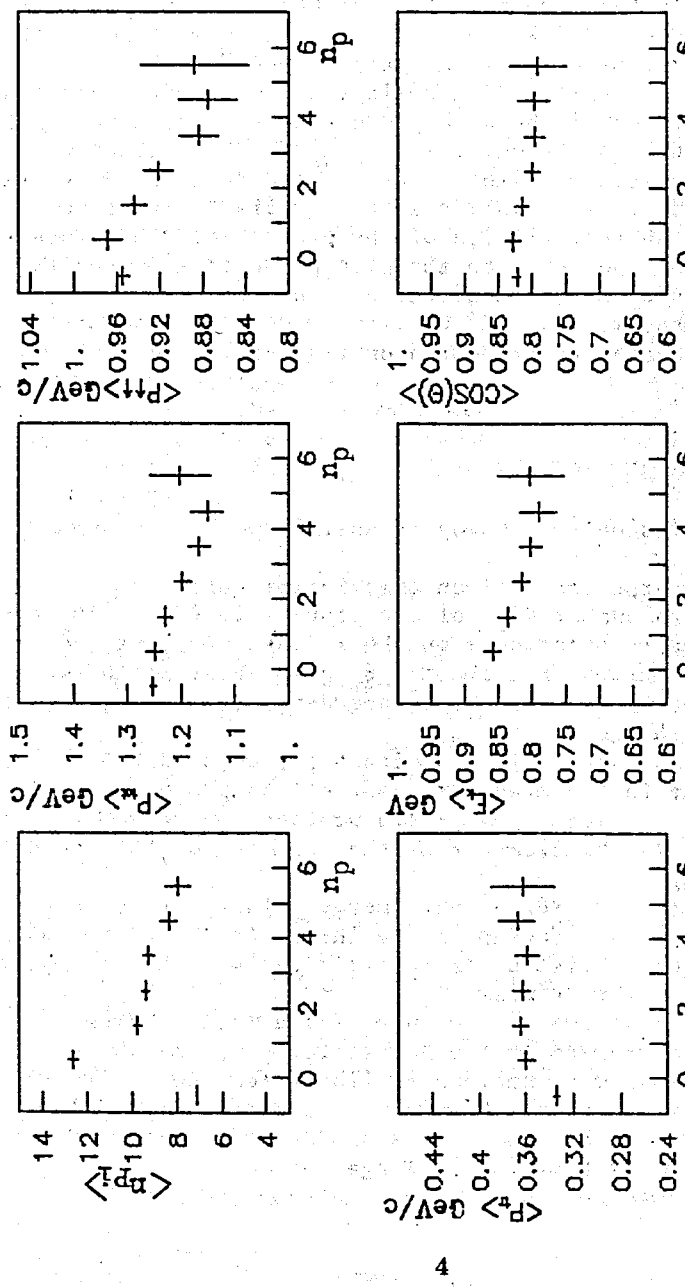


Fig. 1. The mean multiplicity  $\langle n_{\pi} \rangle$ , mean total  $\langle p_{\text{tot}} \rangle$ , longitudinal  $\langle p_{\text{long}} \rangle$ , and transversal  $\langle p_{\text{tr}} \rangle$  momenta, and mean kinetic energy  $\langle E_k \rangle$ , and mean  $\langle \cos\theta \rangle$  of the pions ejected in  $\pi^- + {}^{12}\text{C}_6$  nuclear collisions at 40  $\text{GeV}/c$  momentum, in dependence on the number  $n_{\pi}$  of the protons emitted from the target nucleus in the collision reaction.

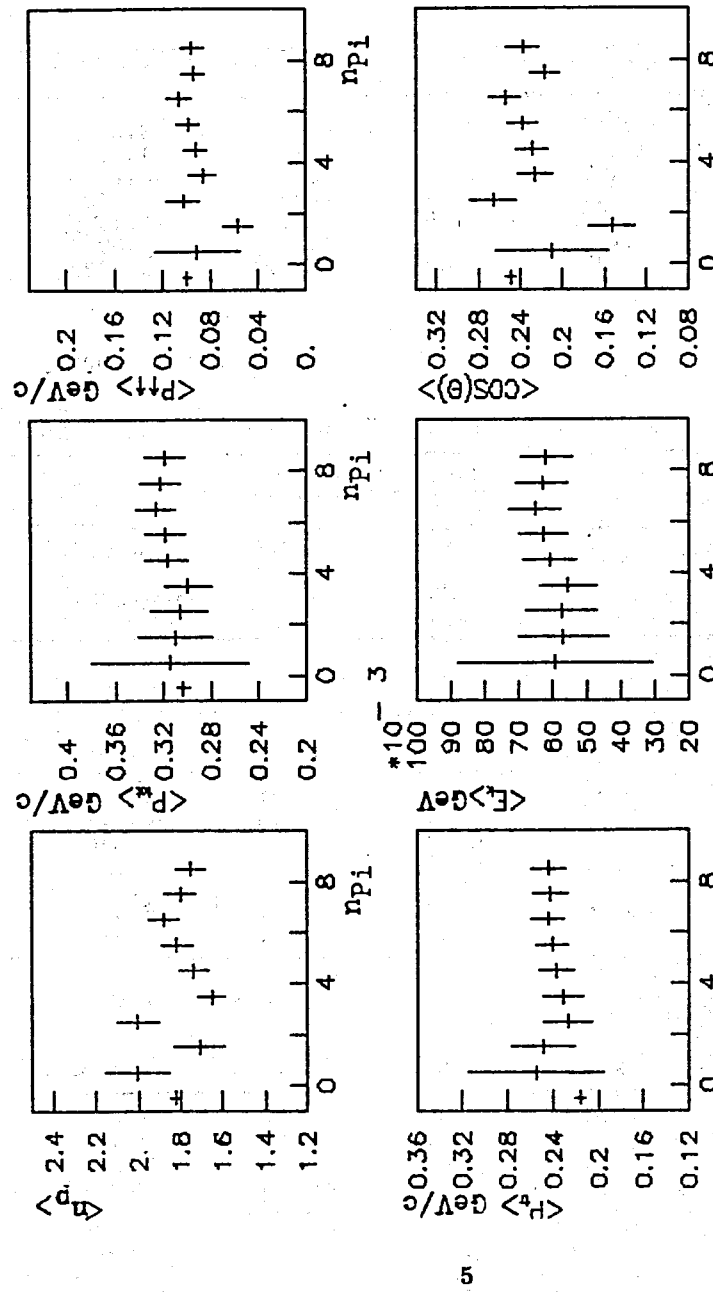


Fig. 2. The mean multiplicity  $\langle n_{\pi} \rangle$ , mean total  $\langle p_{\text{tot}} \rangle$ , longitudinal  $\langle p_{\text{long}} \rangle$ , and transversal  $\langle p_{\text{tr}} \rangle$  momenta, and mean kinetic energy  $\langle E_k \rangle$ , and mean  $\langle \cos\theta \rangle$  of the pions emitted in  $\pi^- + {}^{12}\text{C}_6$  nuclear collisions at 40  $\text{GeV}/c$  momentum, in dependence on the multiplicity  $n_{\pi}$  of the pions ejected in the collision reactions.

Table I. The characteristics of the distributions shown in fig.1

$n_p$	$N_{ev}$	$\langle n_{ri} \rangle$	s.d.	skewness	kurtosis
$\geq 0$	3574	7.14	3.72	0.7056	0.8929
0	252	12.66	2.75	1.1986	1.1509
1	459	9.77	4.99	-0.2937	-0.2748
2	400	9.41	5.16	-0.1149	-0.6723
3	160	9.28	4.78	-0.1629	-1.4175
4	73	8.35	4.17	0.2262	-1.0914
5	28	7.96	3.02	0.4220	-0.5735

Table II. The characteristics of the distributions shown in fig.1

$n_p$	$\sum N_{Pi}$	$\langle P_{tot} \rangle$	s.d.	skewness	kurtosis
$\geq 0$	41706	1.25	1.00	0.9452	-0.0532
0	5943	0.96	0.98	0.9799	0.0403
1	7919	1.23	0.97	1.0237	0.1476
2	5636	1.20	0.96	1.0287	0.1394
3	3058	1.17	0.96	1.1169	0.3972
4	1350	1.15	0.96	1.1298	0.3969
5	390	1.20	1.02	0.9735	-0.1091

Table III. The characteristics of the distributions shown in fig.1

$n_p$	$\sum N_{Pi}$	$\langle P_{lon} \rangle$	s.d.	skewness	kurtosis
$\geq 0$	38395	0.95	0.82	0.7226	-0.4180
0	5506	0.97	0.80	0.7361	-0.3696
1	7351	0.94	0.80	0.7683	-0.3189
2	5267	0.92	0.81	0.7903	-0.3068
3	2860	0.88	0.79	0.8410	-0.2094
4	1264	0.88	0.79	0.8951	-0.6688
5	358	0.89	0.84	0.8462	-0.4219

Table IV. The characteristics of the distributions shown in fig.1

$n_p$	$\sum N_{Pi}$	$\langle P_{tr} \rangle$	s.d.	skewness	kurtosis
$\geq 0$	53781	0.33	0.32	2.3560	9.8798
0	7068	0.36	0.29	2.6807	15.3892
1	9516	0.36	0.31	2.8309	16.3275
2	6840	0.36	0.29	2.1570	8.6440
3	3681	0.36	0.29	2.5168	14.7945
4	1652	0.37	0.31	2.6932	14.0877
5	490	0.36	0.30	2.0698	7.0520

Table V. The characteristics of the distributions shown in fig.1

$n_p$	$\sum N_{Pi}$	$\langle E_k \rangle$	s.d.	skewness	kurtosis
$\geq 0$	40030	1.27	0.58	0.2661	-0.8625
0	5232	0.86	0.65	0.7694	-0.4138
1	6990	0.84	0.65	0.7868	-0.4097
2	4996	0.82	0.65	0.8367	-0.3371
3	2742	0.80	0.65	0.8700	-0.2888
4	1212	0.79	0.64	0.9064	-0.1635
5	343	0.80	0.70	0.9086	-0.3725

Table VI. The characteristics of the distributions shown in fig.1

$n_p$	$\sum N_{Pi}$	$\langle \cos \theta \rangle$	s.d.	skewness	kurtosis
$\geq 0$	53666	0.8227	0.3393	-3.2949	11.2350
0	7077	0.8274	0.3056	-3.2599	11.3662
1	9522	0.8152	0.3239	-3.0462	9.6158
2	6842	0.7996	0.3494	-2.8728	8.2279
3	3682	0.7960	0.3477	-2.8124	7.9062
4	1653	0.7978	0.3486	-2.9747	9.0386
5	490	0.7917	0.3558	-2.8612	8.4308

Table VII. The characteristics of the distributions shown in fig.2

$n_p$	$N_{ev}$	$\langle n_p \rangle$	s.d.	skewness	kurtosis
$\geq 0$	3586	1.82	1.14	0.9179	0.9223
0	88	2.00	0.52	0.0472	-1.8441
1	122	1.71	0.89	1.0835	1.7522
2	199	2.00	1.09	0.5248	-0.1566
3	368	1.65	0.92	0.7496	0.4080
4	362	1.74	1.23	1.1123	0.8108
5	342	1.81	1.28	1.4360	2.7237
6	360	1.88	1.22	0.7681	0.1268
7	342	1.80	1.16	0.9852	1.0313
8	364	1.76	1.20	0.9137	0.7193

Table VIII. The characteristics of the distributions shown in fig.2

$n_{Pi}$	$\sum n_p$	$\langle p_{tot} \rangle$	s.d.	skewness	kurtosis
≥ 0	10776	0.303	0.175	1.0822	1.1185
0	73	0.314	0.146	1.4592	2.6342
1	331	0.310	0.136	1.4462	2.6926
2	538	0.306	0.146	1.6173	3.2254
3	805	0.300	0.142	1.6160	3.5355
4	1011	0.317	0.151	1.4357	2.5744
5	1204	0.319	0.151	1.2870	1.7482
6	1201	0.326	0.156	1.3227	1.6942
7	1098	0.322	0.151	1.3024	1.7454
8	1071	0.318	0.147	1.2145	1.5160

Table IX. The characteristics of the distributions shown in fig.2

$n_{Pi}$	$\sum n_p$	$\langle p_{ion} \rangle$	s.d.	skewness	kurtosis
≥ 0	10810	0.099	0.200	0.5131	0.9280
0	73	0.091	0.168	1.2025	3.4584
1	331	0.057	0.188	0.5031	1.6433
2	538	0.102	0.200	0.4478	1.3222
3	806	0.087	0.190	0.6048	1.1778
4	1012	0.093	0.209	0.4468	0.7814
5	1206	0.098	0.208	0.4970	0.8982
6	1201	0.106	0.213	0.4946	0.8455
7	1099	0.094	0.213	0.5206	0.9548
8	1072	0.095	0.199	0.4162	0.9681

Table X. The characteristics of the distributions shown in fig.2

$n_{Pi}$	$\sum n_p$	$\langle p_{tr} \rangle$	s.d.	skewness	kurtosis
≥ 0	10001	0.216	0.159	1.2751	1.9515
0	73	0.255	0.129	1.0798	2.0894
1	331	0.249	0.120	1.1238	2.6405
2	538	0.227	0.119	1.2480	2.6815
3	806	0.231	0.122	1.3897	3.6418
4	1012	0.237	0.126	1.3290	0.0315
5	1206	0.241	0.127	1.1945	1.9914
6	1204	0.243	0.125	1.1431	1.7403
7	1099	0.243	0.123	1.1296	2.0242
8	1072	0.244	0.126	1.1770	2.5398

Table XI. The characteristics of the distributions shown in fig.2

$n_{Pi}$	$\sum n_p$	$\langle E_k \rangle$	s.d.	skewness	kurtosis
≥ 0	9990	0.249	0.109	1.2751	1.9515
0	73	0.059	0.059	2.5338	8.0168
1	331	0.057	0.055	2.5137	8.3065
2	538	0.057	0.060	2.6327	8.6672
3	806	0.055	0.059	3.0159	12.4417
4	1011	0.061	0.062	2.5829	8.8709
5	1206	0.063	0.064	2.4474	8.0907
6	1201	0.065	0.065	2.1392	5.1377
7	1099	0.063	0.063	2.2745	6.6757
8	1072	0.062	0.060	2.2105	6.5737

Table XII. The characteristics of the distributions shown in fig.2

$n_{Pi}$	$\sum n_p$	$\langle \cos \theta \rangle$	s.d.	skewness	kurtosis
≥ 0	10815	0.2487	0.5890	-0.5521	-0.8506
0	73	0.2104	0.4837	-0.5600	-0.3588
1	331	0.1527	0.5098	-0.1648	-0.9278
2	538	0.2660	0.5360	-0.5392	-0.8338
3	806	0.2263	0.5288	-0.4164	-0.8481
4	1017	0.2285	0.5462	-0.5209	-0.7521
5	1206	0.2371	0.5362	-0.4775	-0.8148
6	1204	0.2548	0.5323	-0.5516	-0.6946
7	1099	0.2166	0.5429	-0.4571	-0.8459
8	1072	0.2381	0.5229	-0.4765	-0.7657

1. The momentum of the produced pions and their kinetic energy mean values decrease slowly with the increasing of the number  $n_p$  of the emitted protons in the collision reactions; to larger numbers of the emitted nucleons larger thicknesses of the intranuclear matter layers involved in the collisions correspond<sup>3,4/</sup>. The pion longitudinal momentum mean value decrease corresponding to the proton multiplicity increase  $\langle n_p \rangle = 5$  amounts about  $\langle p_{long} \rangle \approx 100$  MeV.

2. The transversal momentum of the produced pions does not depend on the number  $n_p$  of the protons emitted in the nuclear collision reactions.

3. The mean number  $\langle n_{Pi} \rangle$  of the produced pions decreases with the  $n_p$  increase - from  $\langle n_{Pi} \rangle \approx 12$  at  $n_p = 0$  up to about  $\langle n_{Pi} \rangle \approx 8$  at  $n_p = 5$ .

4. The mean value  $\langle \cos \theta \rangle$ , for the pion ejection angle  $\theta$ , does not depend on  $n_p$  at  $n_p \geq 2$ .

And so, we do not observe the influence of the pion production process on the characteristics of the proton emission process in pion-nucleus collision reactions at 40 GeV/c momentum.

## REFERENCES

1. Strugalski Z., Sultanov M. - JINR Communication E1-92-68, Dubna, 1992.
2. Strugalski Z., Sultanov M. - JINR Communication E1-92-69, Dubna, 1992.
3. Strugalski Z. - JINR Communication E1-81-576, E1-81-577, Dubna, 1981.
4. Strugalski Z. et al. - JINR Communication E1-90-459, Dubna, 1990.
5. Abdurakhimov A.U. et al - JINR Communication I-6967, Dubna, 1973.
6. Abdurakhimov A.U. et al. - Sov. Journ. for Nuclear Phys., 1973, 18, p.545.

Стругальски З. и др.

Средние характеристики процессов рождения пионов и испускания нуклонов в  $\pi^-$ -C-столкновениях при импульсе 40 ГэВ/с

Получены характеристики процессов рождения пионов и испускания протонов в пион-углерод ядерных столкновениях при 40 ГэВ/с. Средние множественности, средние импульсы и кинетические энергии, и средние углы испускания протонов не зависят от множественности рождения пионов. Средние импульсы и энергии рожденных пионов уменьшаются медленно с ростом множественности испускания протонов.

Работа выполнена в Лаборатории высоких энергий ОИЯИ.

Сообщение Объединенного института ядерных исследований. Дубна 1992

Strugalski Z. et al.

The Mean Characteristics of the Pion Production and Nucleon Emission Processes in Pion-Carbon Nuclear Collisions at 40 GeV/c Momentum

Characteristics of the proton emission and pion production processes are obtained experimentally in pion-carbon nuclear collisions at 40 GeV/c momentum. The mean multiplicities, mean momenta and kinetic energies, and the mean emission angles of the protons do not depend on the intensity of the produced pions. Mean momentum and energy values of the produced pions decrease slowly with increase of the multiplicity of the emitted protons.

The investigation has been performed at the Laboratory of High Energies, JINR.

Communication of the Joint Institute for Nuclear Research. Dubna 1992